Pharmaceutical Research, Vol. 25, No. 10, October 2008 (© 2008)
DOI: 10.1007/s11095-008-9613-4

Research Paper

Investigations on the Humidity-Induced Transformations of Salbutamol Sulphate Particles Coated with L-Leucine

Janne Raula,[1,7] Frank Thielmann,[2] Jarno Kansikas,[3] Sami Hietala,[4] Minna Annala,[5] Jukka Seppälä,[5] Anna Lähde,[1] and Esko I. Kauppinen[1,6]

Received December 4, 2007; accepted April 28, 2008; published online June 27, 2008

Purpose. The crystallization and structural integrity of micron-sized inhalable salbutamol sulphate particles coated with L-leucine by different methods are investigated at different humidities. The influence of the L-leucine coating on the crystallization of salbutamol sulphate beneath the coating layer is explored.

Methods. The coated particles are prepared by an aerosol flow reactor method, the formation of the L-leucine coating being controlled by the saturation conditions of the L-leucine. The coating is formed by solute diffusion within a droplet and/or by vapour deposition of L-leucine. The powders are humidified at 0%, 44%, 65% and 75% of relative humidity and the changes in physical properties of the powders are investigated with dynamic vapour sorption analysis (DVS), a differential scanning calorimeter (DSC), and a scanning electron microscope (SEM).

Results. Visual observation show that all the coated particles preserve their structural integrity whereas uncoated salbutamol sulphate particles are unstable at 65% of relative humidity. The coating layer formed by diffusion performs best in terms of its physical stability against moisture and moisture-induced crystallization. The degree of crystallization of salbutamol in the as-prepared powders is within the range 24–35%. The maximum degree of crystallization after drying ranges from 55 to 73% when the salbutamol crystallizes with the aid of moisture. In addition to providing protection against moisture, the L-leucine coating also stabilizes the particle structure against heat at temperatures up to 250°C.

Conclusion. In order to preserve good flowability together with good physical stability, the best coating would contain two L-leucine layers, the inner layer being formed by diffusion (physical stability) and the outer layer by vapour deposition (flowability).

KEY WORDS: crystallization; humidity; L-leucine coating; salbutamol sulphate; stability.

INTRODUCTION

The crystalline form of a drug is of great importance for maintaining its chemical and physical stability during storage. Although an amorphous material as compared to the corresponding crystalline state shows enhanced dissolution and bioavailability due to the high internal energy and specific volume, it may convert to the crystalline state either spontaneously and/or with the aid of external stimuli (1–3). An amorphous material is thermodynamically metastable, which may, during processing or in the final dosage form, cause instability of drug release and dosing as a result of phase transformation (4). This should be taken into account, especially in humid conditions, since an amorphous material is usually notably more hygroscopic than its crystalline form. However, the crystallization of an amorphous material can conventionally be prevented by storing it below the glass-transition temperature (T_g), by avoiding exposure to moisture or by elevating the T_g of the system with the aid of added excipients (5–7). Therefore, it is of the utmost importance to control the crystalline form of the drug during the various stages of its development and storage.

Various pharmaceutical formulation techniques, such as drug polymorphs, solvates and phase transitions, significantly affect the final crystalline form of a drug. For instance, spray-drying (8,9) and lyophilisation (10) processes often lead to the formation of the amorphous form of a drug. Also processes such as grinding, milling, granulation, drying, precipitation and compaction, in which stress is applied to large crystals, may result in a fractionation of the amorphous state. This may cause instability problems, such as polymorphic changes and the

[1] NanoMaterials Group, Laboratory of Physics and Center for New Materials, Helsinki University of Technology (TKK), P.O. Box 5100, 02015 TKK, Finland.
[2] Surface Measurement Systems Ltd., 3 Warple Mews, Warple Way, London W3 0RF, UK.
[3] Laboratory of Inorganic Chemistry, University of Helsinki, P.O. Box 55, Helsinki 00014, Finland.
[4] Laboratory of Polymer Chemistry, University of Helsinki, P.O. Box 55, Helsinki 00014, Finland.
[5] Laboratory of Polymer Technology, Helsinki University of Technology (TKK), P.O. Box 6100, 02015 TKK, Finland.
[6] VTT Biotechnology (VTT), P.O. Box 1000, 02044, Espoo Finland.
[7] To whom correspondence should be addressed. (e-mail: janne.raula@tkk.fi)

agglomeration of the micronized drug (11,12). The latter may, even to a small extent, cause dosing problems for inhalable powders. For deep lung delivery of fine particles, possible agglomerates must be broken down to individual particles whose size is within the respirable range, i.e. less than 5 μm. Instead of attempting to crystallize a drug during its formation process (13–15), the drug formulation may be post-treated by moisture or heat (1,16–18). The post-treatment of a powder, however, often results in sintering of the particles due to the increased mobility of molecules of amorphous particle surfaces (19). This sintering can be avoided by covering the amorphous or molten material with a protective layer during treatment (20).

We have developed a novel way of preparing drug particles by simultaneously coating them with the amino acid L-leucine via physical vapour deposition (21). In practice, droplets containing both the drug and L-leucine are dried, when the L-leucine molecules, which possess surface activity toward an air–water interface (22,23), formed an outer layer on the core drug particles. Within a single heat cycle, L-leucine evaporates from and nucleates onto the core surfaces. During deposition, the L-leucine forms a solid coating layer consisting of leafy looking crystals pointing out of the core surface. The structure of the coating could be controlled by the degree of saturation of the L-leucine. All the powders where salbutamol sulphate cores were coated via L-leucine vapour exhibited excellent flow and gas-phase dispersion characteristics (24).

It is obvious that the structure and state of the coating layer are critical for stabilizing the core particles under different environmental conditions. Thus, our work aims to explore the influence of moisture on (1) the morphological stability of uncoated salbutamol particles and those coated with L-leucine in different ways, and (2) the salbutamol crystallization beneath the coating layer. Humidity-induced transformations of salbutamol, such as amorphous–crystalline transitions, and the particle morphology have also been investigated.

MATERIALS AND METHODS

Precursor Solutions

Salbutamol sulphate, S, (Alfa Aesar, Germany) and amino acid L-leucine, L, (Fluka, Switzerland) were used as received. Materials were dissolved in deionized water (pH 6; Millipore) to give precursor solutions in which the concentration of salbutamol was 30 g/l and that of L-leucine 7.5 g/l. The salts used to prepare saturated solutions for tests at different relative humidities were potassium carbonate (Aldrich, Germany), sodium nitrite (Merck, Germany), and NaCl (Riedel-de-Haën, Germany).

Preparation of Coated Powders

The simultaneous production and gas-phase coating of solid salbutamol sulphate particles with L-leucine has been discussed in detail in our previous work (21). Particle preparation in the aerosol flow reactor (25,26) consists of the generation of droplets, drying of particles, and coating of dry solid particles via the physical vapour deposition (PVD) of L-leucine. Solute droplets from the precursor solutions were formed using an ultrasonic nebulizer (RBI Pyrosol 7901, France) equipped with an internal water circulator to keep the temperature of the solutions constant at 20 (±1)°C. The reactor has been modified for scaling-up the production in the following way. The solute droplets generated with a solution consumption of 101 ml/h were transferred with the aid of dry nitrogen gas [10.0 (±0.1) l/min, 22°C] into the heated part of the reactor consisting of five stainless steel tubes (ID 3 cm, length 120 cm). This resulted in a gas-phase concentration of 1.25 g/m^3 for L-leucine in each reactor tube, the flow rate being 2.0 l/min. The tubes were placed in a special oven designed by Meyer Vastus (Finland) where the temperature was controlled by three separate heaters. Experiments were carried out at temperatures of 100°C, 160°C and 190°C (±1°C), measured in the middle of the reactor tubes with a K-type thermocouple. The residence time of particles in the heated section, where the flow was laminar, ranged from 21 to 17 s at temperatures from 100 to 190°C, respectively. The tubes were merged together just before a section where the particles were rapidly cooled with dry nitrogen gas (22°C) by a volume ratio of 8:1 in a porous stainless steel tube (ID 3 cm, length 20 cm). In this part, the flow was turbulent with a Reynolds number over 3000. The cooling rates ranged from 0.9 to 2.2°C/ms when the temperature decreased from 100°C or 190°C to 30°C, respectively. In addition to cooling, the large gas volume minimized water re-condensation and particle deposition on the walls of the stainless steel aerosol mixing tube (ID 3 cm, length 55 cm) prior to particle sampling. The particles were collected by a small-scale cyclone (27) with a nominal cut-off diameter (D50) of 0.65 μm at the 90 l/min as used in this work.

Vapour Conditions in the Reactor

The sublimation temperature and the saturation ratio of L-leucine were estimated using the enthalpy of sublimation (ΔH_{sub}=150.7 kJ/mol at T_{sub}=455 K) according to a previous study (28) in the following way. The saturation vapour pressure (p_s) was calculated using the equation

$$p_s = p^* e^{-C} \text{ with } C = \frac{\Delta H_{sub}}{R}\left(\frac{1}{T_R} - \frac{1}{T^*}\right), \quad (1)$$

where p^* is the vapour pressure at the temperature T^*, T_R is the reactor temperature, and R is the gas constant. The vapour pressure (p) of L-leucine in the reactor was calculated using the equation

$$p = \frac{qRT_R}{MQ_R} \text{ with } Q_R = Q_{293K}\left(\frac{T_R}{293\,K}\right), \quad (2)$$

where q is the mass consumption of L-leucine by the reactor (g/min), M is the molecular weight of L-leucine, and Q_R is the flow rate in the reactor at a certain temperature. Q_R is corrected with respect to temperature using the above relation where $Q_{293\ K}$ is 2.0 l/min. The saturation ratio was estimated according to the relation

$$S = \frac{p}{p_s}. \quad (3)$$

The rapid cooling induced a sudden change in the saturation conditions, causing the L-leucine vapour to supersaturate and resulting in the saturation ratio being temporarily far above unity ($>1\times10^7$). The saturation ratio of water was below zero (<0.01 at 30°C) calculated using the saturation vapour pressures given in the literature (29).

Instrumentation and Characterization

The number size distributions of the produced particles were determined with an electrical low-pressure impactor, ELPI, (Dekati Ltd., Finland). Oiled porous collection substrates (Dekati Ltd., Finland) with stage aerodynamic cut-off diameters from 0.03 to 7.88 μm were used to avoid particle bounce. The density of all the particles was assumed to be 1 g/cm^3. The particle geometric number mean diameter (GNMD) and geometric standard deviation (GSD) of the size distribution were defined as

$$\mathrm{GNMD} = \exp\left(\frac{\sum n_i \ln D_i}{N}\right), \text{and} \tag{4}$$

$$\mathrm{GSD} = \exp\left(\left(\frac{\sum n_i (\ln D_i - \ln\ \mathrm{GNMD})^2}{N-1}\right)^{1/2}\right), \tag{5}$$

where n_i is the number of particles in the ith size stage, D_i is the aerodynamic diameter of the ith size stage, and N is the total number of particles, i.e. $\sum n_i$.

The morphology of the particles was imaged with a field-emission scanning electron microscope, FE-SEM (Leo DSM982 Gemini, LEO Electron Microscopy Inc., Germany). The samples were coated with sputtered platinum in order to stabilize them under the electron beam and to enhance image contrast.

The powder compositions were determined by a nuclear magnetic resonance (NMR) spectrometer. Proton NMR measurements were conducted with a 200 MHz Varian Gemini 2000 spectrometer using deuterated water as the solvent. The characteristic chemical shifts used for salbutamol sulphate were 6.8–7.4 ppm (3H, phenyl protons) and for L-leucine 0.8–1.0 ppm (6H, methyl protons).

The particle crystallinity before humidification was analysed by X-ray diffraction (XRD; control unit Philips PW 1710, goniometer Philips PW 1820, generator Philips PW 1830, The Netherlands). CuKα radiation (40 kV, 50 mA, with wavelengths $K\alpha_1$ of 0.154060 nm and $K\alpha_2$ of 0.154439 nm, with an α_1/α_2 intensity ratio of 0.5) was used. The XRD patterns were recorded at diffraction angles from 3° to 40° in 2θ using a step size of 0.02° and a scan speed of 0.004° 2θ/s. The particle crystallinity after humidification was analysed by PANalytical X'Pert Pro MPD X-ray diffraction system (The Netherlands). CuKα radiation (45 kV, 40 mA, with the wavelengths $K\alpha_1$ of 0.154060 nm, $K\alpha_2$ of 0.154443 nm and a $K\alpha_1/K\alpha_2$ intensity ratio of 0.5) was used. The XRD patterns were recorded at diffraction angles from 5° to 45° in 2θ with the PIXcel detector using a step size of 0.0070° in 2θ and scan step time of 52.7513 s in continuous scanning mode with a PSD length of 3.35° in 2θ. Divergence slit used was 0.25° and scattering slit 0.5°.

The particle surface was analysed with X-ray photon spectroscopy, XPS (AXIS 165, Kratos Analytical Ltd., UK). The elements O (total of all orbitals), C (1*s* orbital), N (1s orbital), and S (2*p* orbital) were used for the elemental analysis.

Dynamic vapour sorption experiments were performed on a DVS-1 automated gravimetric vapour sorption analyser (Surface Measurement Systems Ltd., London, UK). The DVS-1 measures the uptake and loss of vapour gravimetrically using a Cahn D200 recording ultra-microbalance with a mass resolution of ±0.1 μg. The relative concentration around the sample was controlled by mixing saturated and dry carrier gas streams using mass-flow controllers. The measurement temperature was maintained constant at 25.0 (±0.1)°C by enclosing the entire system in a temperature-controlled incubator. For the water uptake experiments a mass of 20 mg was loaded into a sample cup and placed in the system. Prior to being exposed to any vapour, the samples were equilibrated for a short period of time at 0% RH to remove any surface water present and establish a dry, baseline mass. The samples were exposed to the following concentration profile: 0 to 10% in 1% steps, 20% to 90% in 10% steps, 95%, and the same for desorption. At each stage, the sample mass was allowed to reach equilibrium before the partial pressure was increased or decreased. An isotherm was calculated from the complete sorption and desorption profile using the DVS Advanced Analysis Suite v3.6.

Calorimetric measurements were conducted using differential scanning calorimetry, DSC (Mettler Toledo DSC 821) in a gaseous nitrogen atmosphere. The samples were heated from 25°C to 250°C with a heating rate of 10°C/min.

Salbutamol sulphate was analysed by a liquid chromatography-mass spectrometry (LC-MS). In LC (Acquity Ultra Performance LC, Waters), it was employed a mixture of methanol and 0.1% *w/w* aqueous ammonium acetate (45:55, pH 4.5) as a mobile phase running at a flow rate of 0.25 ml/min. The column was Acquity UPLC C18; 1.0×5.9; 1.7 μl that was operated at 40°C. MS used was LCT Premier MS (Micromass).

Equilibrium water uptake measurements were conducted in desiccators where 44%, 65%, and 75% relative humidity (RH) were achieved with saturated solutions of the salts Na_2NO_2, K_2CO_3, and NaCl at 25°C, respectively. The samples regarded as 0% RH or non-conditioned were stored over silica in the desiccator, where the humidity was 0–1% RH. The samples under humidification, i.e. conditioned samples, were investigated with SEM and DSC after 2 and 7 days. DSC runs were performed on the samples as soon as they were removed from the humidity chamber and also after drying over silica for 5 days.

RESULTS AND DISCUSSION

Particle Preparation

Table I shows the main experimental details of the particle preparation and some characteristics of the resulting particles. The saturation conditions of L-leucine in the reactor for coating the salbutamol core particles were selected in the

Table I. The Experimental Conditions of Particle Synthesis and Characteristics of the Particles

	Precursor solutions			Particle preparation				Produced particles			
Sample	C_{total} (g/l)	S (wt%)	L (w%)	T_{heat} (°C)	Saturation ratio	v_{cool} (°C/ms)	Way of coating	GNMD (μm)	GSD	S (wt%)	L (wt%)
S100–100	30.0	100	0	100	–	0.9	–	0.9	2.9	100	0
S89L11–100	37.5	80	20	100	1 (8,270)	0.9	(1)	1.0	2.8	89	11
S91L09–160	37.5	80	20	160	1 (8.6)	1.8	(1)+(2)	n.a.	n.a.	91	9
S95L05–190	37.5	80	20	190	0.5	2.2	(2)	n.a.	n.a.	95	5

The saturation ratios shown in the parentheses are those of the momentary supersaturation calculated using Eqs. 1, 2 and 3. The methods of L-leucine coating are (1) diffusion to particle surface and (2) physical vapour deposition.
S Salbutamol sulphate, *L* L-leucine, C_{total} total solution concentration, T_{heat} temperature in the heated section, v_{cool} the cooling rate of aerosol, *GNMD* geometric number mean diameter, *GSD* geometric standard deviation, *n.a.* not applicable

following way. At 100°C L-leucine did not evaporate and remained in the condensed phase during particle formation. The coating was formed by the diffusion of L-leucine onto the droplet surface prior to drying. Thus, the resulting dry particles should contain the same amount of material as in the corresponding precursor solution. However, this is not the case with the sample S89L11–100. This could be explained by the formation of small droplets consisting mainly of L-leucine. Since L-leucine is a surface-active molecule, it enriches on the air–water surface of the precursor solution where droplets are formed. This lowers surface tension resulting in a decreased droplet size (30). The resulting small particles were removed upon cyclone collection (cut-off ~0.65 μm). The conditions at 160°C favoured L-leucine saturation when estimated using Eqs. 1, 2, and 3. However, we observed in our earlier study (21) that the sublimation temperature of L-leucine from the surface of salbutamol particles was approximately 150 (±5)°C. In this case the coating was formed both by surface diffusion, as at 100°C, and via the heterogeneous nucleation of L-leucine vapour on the core particle surfaces. At 190°C L-leucine fully sublimed and the coating was formed purely via the heterogeneous surface nucleation of L-leucine. In addition, pure L-leucine particles were formed via homogeneous nucleation, which was observed as a notable increase in the number of sub-micron particles. Accordingly, the amount of L-leucine on the core particle surface decreased.

Particle Structure

Figure 1 shows the SEM images and schematics of pure salbutamol particles and salbutamol particles with different L-leucine coatings depending on the applied experimental

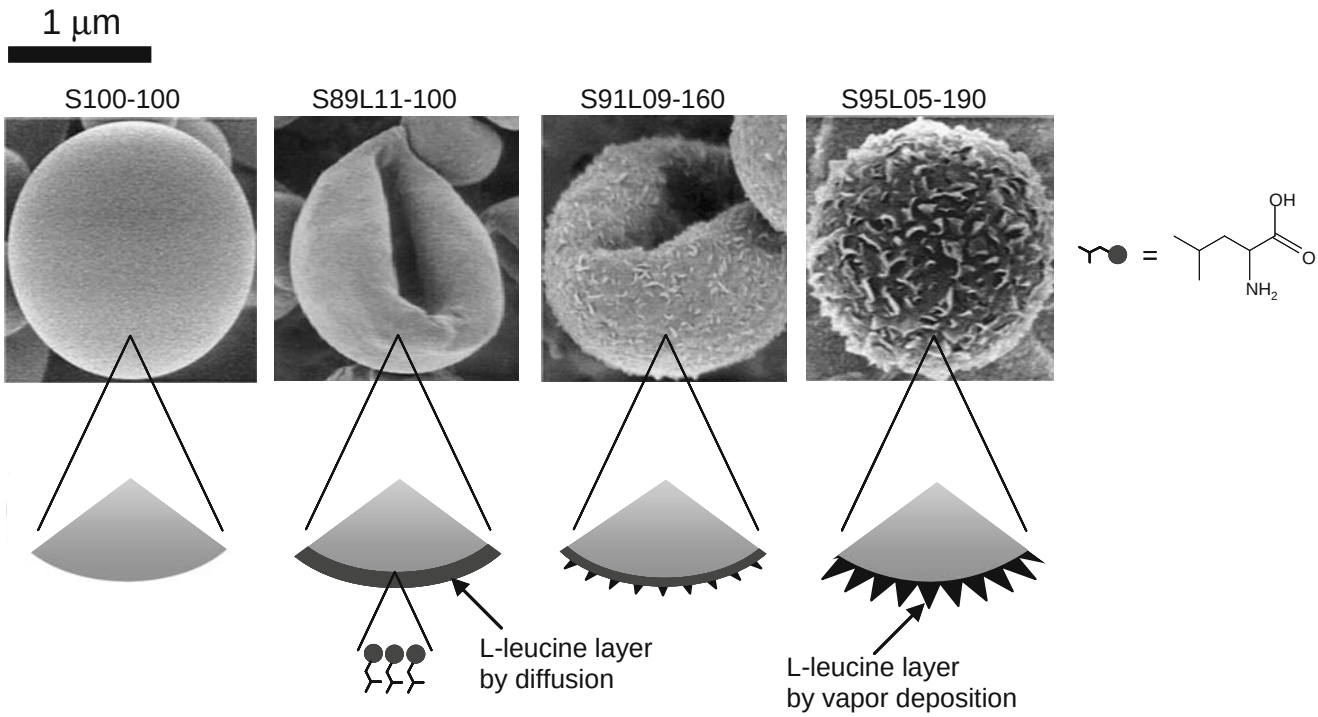

Fig. 1. SEM images of the uncoated salbutamol particles (S100–100) and L-leucine coated salbutamol particles (S89L11–100, S91L09–160, and S95L05–190). Figure also shows the schematics of the particle surfaces where L-leucine layer is formed by different ways i.e. by diffusion during droplet during (S100–100), by the vapour deposition of L-leucine (S95L05–190), or by the combination of these two ways (S91L09–160). The chemical structure of L-leucine and its corresponding caricature are shown on the right. The letters *S* denote to salbutamol sulphate and L to L-leucine. The *figures following the letters* indicate the mass fractions of the compounds. The scale bar is 1 μm.

conditions. The presented schematics are based on our previous study on particle coating (21). Note that the selected individual particles in the figure are approximately the same size in order to demonstrate the differences in particle morphology. In reality, the vapour deposition of L-leucine on particle surfaces depends on the size of the core salbutamol particles according to the relation $dD_p/dt \sim 1/D_p$ (31), where D_p is the particle size and t is time. Thus, the growth rate of particles via heterogeneous nucleation increases, i.e. the coating thickness increases with decreasing size of the core particles. Pure salbutamol particles (S100–100) were spheres whose morphology becomes wrinkled with added L-leucine (S89L11–100). This morphology change has been attributed to the strong enrichment of L-leucine molecules on the droplet surface, which form a film that collapses when water is removed by evaporation (32). The L-leucine molecules assemble on the outer surface of the droplets in such a way that an isobutyl group (hydrophobic) is facing the air phase and an amide group (hydrophilic) is facing the aqueous phase. This molecular orientation remains on the surface of the resulting dry particles. The particles produced at 160°C were wrinkled with L-leucine chips on the surface (S91L09–160). These chips formed during vapour deposition and were proved to be crystalline by XRD and TEM (33). Since L-leucine partially sublimed, two separate L-leucine surface layers were formed: an inner layer by L-leucine diffusion to the droplet surface and an outer layer composed of L-leucine crystals formed by vapour deposition. When L-leucine was fully evaporated at 190°C, the salbutamol particles regained the original spherical shape that they had prior to the nucleation of L-leucine vapour (S95L05–190). This is assumed to be due to the fluidic nature of salbutamol above its glass-transition temperature, which has been reported to be 64°C (19). XPS studies proved a strong enrichment of L-leucine (>90%) on the particle surfaces regardless of the preparation method, see Table II.

XRD studies with pure L-leucine particles have shown that L-leucine has a crystalline structure under any saturation conditions (33). The crystal orientation, however, depends on the preparation method, i.e. droplet drying or vapour deposition. Figures 2 and 3 show the XRD spectra of the bulk powders and prepared salbutamol/L-leucine particles, respectively. Pure salbutamol particles (S100–100) were mainly amorphous, but some diffraction peaks indicating crystallinity were found. The smooth spectra of the salbutamol/L-leucine particles implied that the particles were mostly amorphous. However, some diffraction peaks (001 and −110 for S89L11–100 and S91L09–160, and 001 and 004 for S95L05–190) were most probably due to L-leucine crystals.

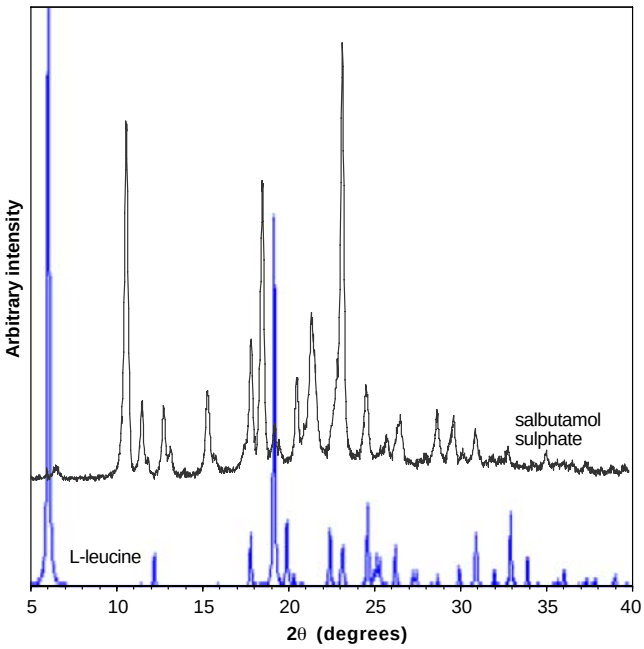

Fig. 2. The XRD spectra of bulk salbutamol sulphate and L-leucine.

Table II. The Elemental Analysis of the Bulk and Produced Powders Conducted with an X-ray Photon Spectrometer (XPS)

	Elements			
Sample	Oxygen %	Carbon %	Nitrogen %	Sulphur %
S (bulk)	24.5 (2.7)	67.6 (0.6)	5.6 (6.8)	2.3 (5.2)
L (bulk)	20.5 (0.3)	68.4 (0.9)	11.1 (5.1)	0.0 (0.0)
S89L11–100	20.4 (0.9)	69.0 (1.4)	10.3 (11.0)	0.3 (12.0)
S91L09–160	21.4 (8.5)	68.3 (2.3)	10.0 (2.9)	0.3 (2.1)
S95L05–190	20.8 (3.7)	69.4 (0.3)	9.6 (5.2)	0.2 (44.8)

Analyses were performed two to three times. Standard deviations are shown in the parentheses.

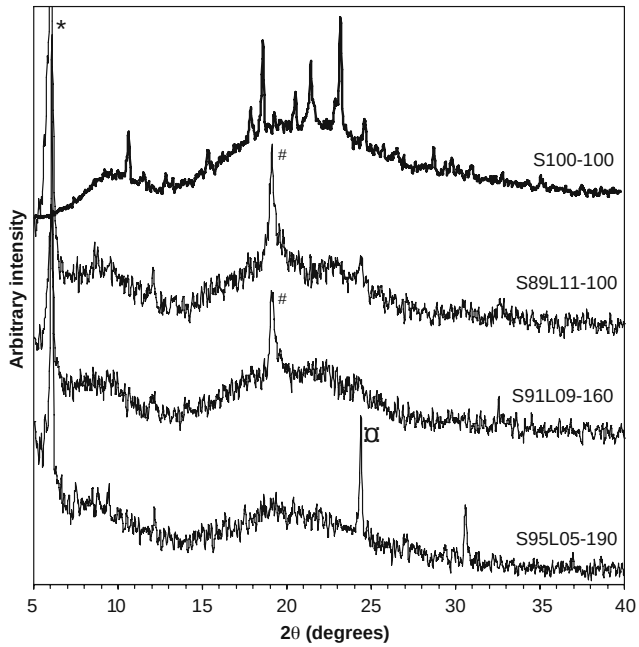

Fig. 3. The XRD spectra of the produced particles S100–100, S89L11–100, S91L09–160, and S95L05–190. The symbols denote to the diffraction peaks: * to 001, # to −110, and ¤ to 004.

Particles Under Humid Conditions

Dynamic Vapour Sorption

Figure 4 shows the water vapour sorption curves of the particles. In the case of S100–100, the water uptake curve of the powder samples increased in an S-shaped manner where the first distinguishable plateau was found at 30–40% RH and the second one at 60–70% RH. One should note that salbutamol sulphate is not hygroscopic and does not form hydrates (34). Burnett *et al.* (35) have studied the glass-transition and crystallization behaviour of spray-dried salbutamol sulphate at varying temperatures and humidities. Accordingly, the first transition at 30–40% RH is attributed to glass transition and the transition at 60–70% RH to crystallization of salbutamol sulphate. However, the water-uptake levels in our study did not agree with their study, which could be due to the different original state of the particles. The water uptake did not increase further, which supports crystallization. Interestingly, water did not desorb when the humidity was decreased but was preserved in the sample even at 0% RH. Columbano *et al.* (34) exposed amorphous spray-dried salbutamol to 75% RH, resulting in a water uptake of ~13 wt%. When the relative humidity was returned to 0%, the water content gradually decreased, but was still 6 wt% after 65 h. They concluded that water was trapped inside the crystalline structure of salbutamol, which inhibited its release.

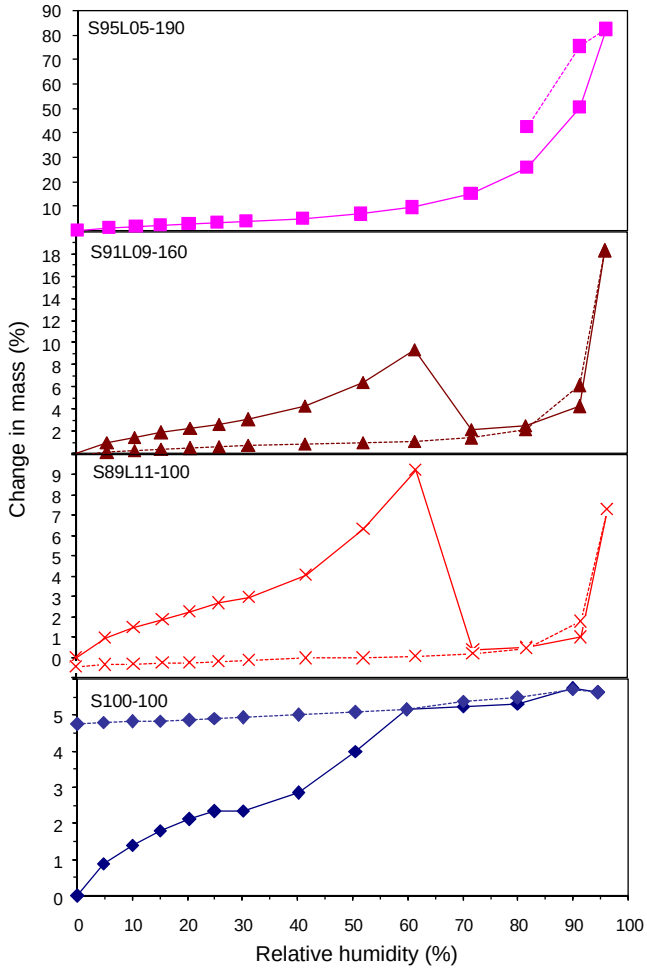

Fig. 4. The sorption curves of water vapour shown as the change in sample mass versus relative humidity. The absorptions are shown as *solid lines* and desorptions as *dashed lines*. Note that the *y*-axis varies in the plots.

All the L-leucine-containing particles showed higher uptake of water than pure salbutamol particles. However, samples S89L11–100 and S91L09–160 showed a sudden decrease in mass within the range 60–70% RH; this was attributed to the crystallization of amorphous salbutamol, which led to water being expelled (36). No crystallization was observed with S95L05–190. Instead, this sample showed a very high water uptake with a mass change of 80% at 96% RH. The issue of why and how the crystallization of salbutamol sulphate depends on the applied L-leucine coating will be discussed later.

Particle Morphology

In general, all the particles remained intact at 44% RH and were agglomerated, i.e. formed bridges and necks with adjacent particles, at 75% RH, see Fig. 5. However, the degree of agglomeration, as visually observed, varied distinctively according to the type of L-leucine coating. Pure salbutamol particles did not agglomerate at 44% RH but at 65% and 75% RH the agglomeration was notable, resulting in large strongly coagulated clumps with no resemblance to the individual particles. Instead, the particles containing L-leucine preserved their morphology well when compared with the uncoated salbutamol particles. Among these particles, the intactness of S89L11–100 particles was seemingly better preserved than that of S91L09–160 and S95L05–190 particles. No particular influence of exposure time on the agglomeration behaviour was observed.

Differential Scanning Calorimetry

Bulk Salbutamol Sulphate and L-leucine Crystalline bulk salbutamol sulphate exhibited a melting endotherm (ΔH −154.0 J/g) with a peak temperature (T_{peak}) of 202°C. Salbutamol sulphate melts with degradation within the broad temperature range 210–350°C (37). L-leucine did not show any distinctive thermal processes within the studied temperature range. There have been various studies on the sublimation and decomposition of L-leucine. For instance, Martins *et al.* (38) found that L-leucine sublimed at 251°C when measured with DSC, whereas the sublimation was observed at 290°C by thermogravimetric analysis (TGA). In contrast, Li *et al.* (39) reported that sublimation took place at 295°C (DSC) followed by decomposition at 303°C (TGA). They also observed that complete mass loss took place in a single step within the temperature range 207–355°C. On the other hand, the sublimation temperature of L-leucine has also been reported to be distinctly lower, 145–148°C (40).We also observed in our previous work that the sublimation of L-leucine from nanoparticles in the gas phase took place markedly below 200°C (33). Moreover, the onset temperature depended on the L-leucine concentration and original particle size. The lower sublimation temperature with gas-borne nanoparticles is justified, because mass and heat transfer in such particles is notably faster than in the bulk material.

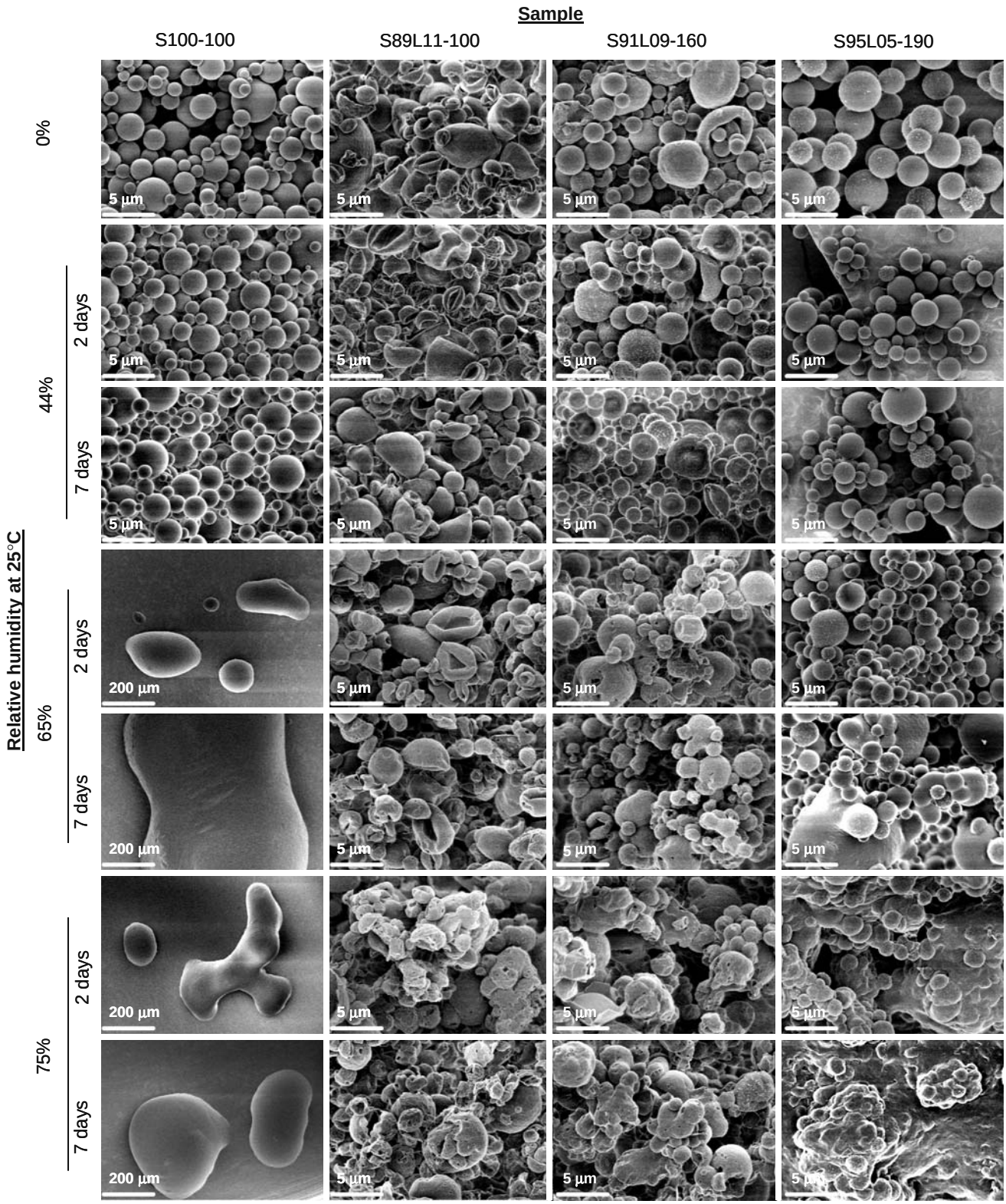

Fig. 5. The SEM images of the non-conditioned (0% RH) and conditioned (44%, 65%, 75% RH) samples. The samples were conditioned 2 and 7 days followed by 5 days drying over silica.

Particles Stored at 0% RH Figure 6 shows the DSC thermographs of the non-conditioned (0% RH) and conditioned (44%, 65%, and 75% RH) samples. All the non-conditioned samples showed a very broad endotherm starting from 50–70°C and ending at approximately 120–125°C that was attributed to the evaporation of absorbed water. The presence of water was proved by heating the samples first to 100°C followed by re-heating from 25 to 250°C, when no

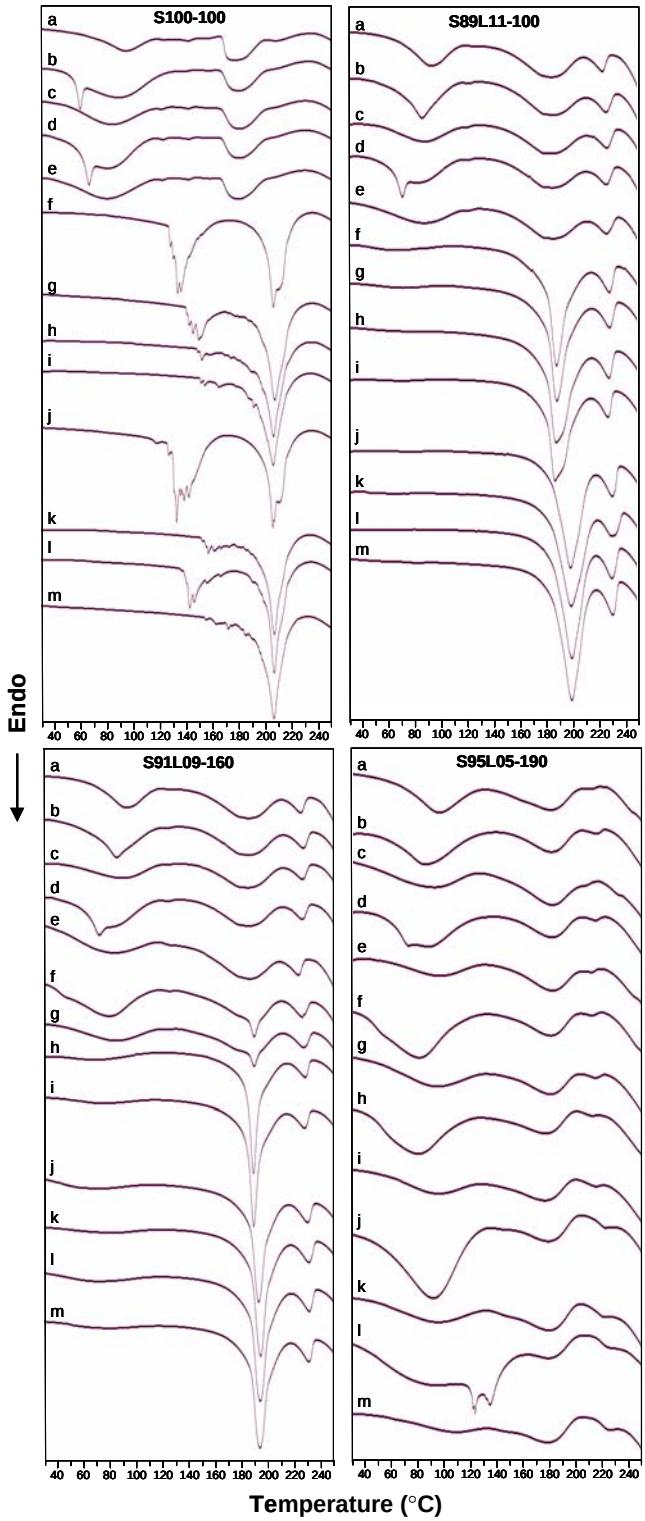

Fig. 6. The DSC thermograms of the humidity conditioned S100–100, S89L11–100, S91L09–160 and S95L05–190 particles: *a* 0% RH; *b* 44% RH, 2 days, moist sample; *c* 44% RH, 2 days, dried sample; *d* 44% RH, 7 days, moist sample; *e* 44% RH, 7 days, dried sample; *f* 65% RH, 2 days, moist sample; *g* 65% RH, 2 days, dried sample; *h* 65% RH, 7 days, moist sample; *i* 65% RH, 7 days, dried sample; *j* 75% RH, 2 days, moist sample; *k* 75% RH, 2 days, dried sample; *l* 75% RH, 7 days, moist sample; *m* 75% RH, 7 days, dried sample.

endotherm due to water appeared. Table III summarizes the DSC results, where the content of absorbed water (water-%) at 50–115°C has been estimated in relation to the heat of evaporation of water at 373.15 K as 2257 J/g (29). The water content varied between 1.5 and 2.8 wt%.

A broad endotherm in the temperature range 130–210°C was attributed to melting of salbutamol. In addition, the melting took place 20–30°C lower than that of the bulk salbutamol. Corrigan *et al.* (41) assumed that the endotherm was a result of the degradation process of salbutamol. We hypothesize, however, that the endotherm is due to the melting of small salbutamol crystalline domains buried in the amorphous matrix. We showed in the earlier study that a drug ketoprofen was 'solubilized' as an amorphous form within amorphous polymer matrix in the 90–120 nm dry particles (42). Also, the particle integrity improved with the increased interaction between the drug and matrix polymer. In the present study, likewise, the small crystalline domains were 'solubilized' by amorphous matrix of the same material. The size-dependent melting of crystals has been intensively studied (20,43–46). In general, the melting temperature decreases and the endotherm is lowered and becomes broader as the crystal size decreases to a few tens of nanometres. Jiang *et al.* (43) stated that organic nanocrystals exhibit superheating and enhanced entropy of melting, since their vibrational spectrum of the surface region differs from that of the bulk and as a result the melting temperature and entropy are reduced. In the present case, the degree of crystallization of a sample can be estimated by relating its fusion heat to that of bulk salbutamol sulphate. Accordingly, the degrees of crystallization (cryst. %) were from 24% to 35%, see Table 3. These crystals were not clearly observed with XRD, since the width of the diffraction peaks of nanosized crystals at wide angles is considerably broadened with decreasing particle size (47).

The L-leucine-containing particles exhibited an endotherm in the range 210–230°C. In our previous publication, we interpreted that the odd sublimation behaviour of L-leucine was a result of an ionic interaction between salbutamol and L-leucine (21). The break-up of an ionic bond, however, requires notably larger amount of energy than applied in this study. As a consequence, the compounds would decompose prior to the breakage of ionic bond. Hence, this endotherm was attributed to the break-up of the hydrogen bonding between the amino group of salbutamol sulphate and carboxylic acid of L-leucine which can be broken at relatively low temperatures.

Particles Stored at 44% RH In general, the water uptake of the particles increased with the humidity level. Pure salbutamol particles showed the highest tendency to absorb water and to retain water after drying. A separate sharp endotherm at ~60°C, which is in the vicinity of the glass-transition temperature, is attributed to an enthalpy relaxation of amorphous material (5,43–46). However, the relaxation peak disappeared upon 5 days drying. No further crystallization occurred in any of the samples and the peak temperatures were the same as those of the 0% RH samples. Only the T_{peak} of S100–100 increased by a few degrees.

Particles Stored at 65% and 75% RH The crystallization of salbutamol in S100–100 developed notably with increasing humidity. The crystallinity degree increased approximately

Table III. Differential Scanning Calorimetry Results of the Particles Scanned after Humidity Treatment both Directly (State is Moist) and after Drying over Silica for 5 days (state is dry)

Sample		S100–100						S89L11–100							
		50–115°C			130–210°C			50–115°C			130–210°C			210–230°C	
RH	Treatment days/state	T (°C)	ΔH (J/g)	Water %	T (°C)	ΔH (J/g)	Cryst. %	T (°C)	ΔH (J/g)	Water %	*T* (°C)	Δ*H* (J/g)	Cryst. %	*T* (°C)	Δ*H* (J/g)
0%	over silica	93	−34.2	1.5	172	−37.1	24.1	89	−50.6	2.2	176	−51.0	33.1	222	−10.9
44%	2/moist	88	−111.8	4.9	179	−34.5	22.4	84	−61.0	2.7	176	−49.7	32.3	223	−10.4
	2/dry	83	−50.3	2.2	177	−33.3	21.6	86	−32.2	1.4	176	−44.7	29.0	224	−10.5
	7/moist	81	−93.7	4.1	177	−31.0	20.1	82	−68.2	3.0	177	−40.1	26.0	223	−9.8
	7/dry	80	−62.3	2.8	177	−34.1	22.1	84	−49.6	2.2	176	−48.6	31.6	224	−10.8
65%	2/moist	–	–	–	202	−106.6	69.2	64	−10.1	0.4	185	−99.1	64.4	224	−13.0
	2/dry	–	–	–	203	−96.8	62.8	–	–	–	186	−87.8	57.0	226	−12.7
	7/moist	–	–	–	202	−104.2	67.6	–	–	–	185	−111.0	72.1	225	−12.2
	7/dry	–	–	–	202	−86.5	56.2	–	–	–	184	−91.2	59.2	225	−11.0
75%	2/moist	–	–	–	202	−108.7	70.5	–	–	–	196	−113.3	73.6	228	−14.4
	2/dry	–	–	–	203	−84.4	54.8	–	–	–	197	−113.1	73.4	229	−13.1
	7/moist	–	–	–	203	−95.0	61.7	–	–	–	197	−117.8	76.5	228	−15.3
	7/dry	–	–	–	203	−103.6	67.2	–	–	–	197	−110.3	71.6	227	−14.4

Sample		S91L09–160								S95L05–190							
		50–115°C			130–210°C			210–230°C		50–115°C			130–210°C			210–230°C	
RH	Treatment days/state	*T* (°C)	Δ*H* (J/g)	Water %	*T* (°C)	Δ*H* (J/g)	Cryst. %	*T* (°C)	Δ*H* (J/g)	*T* (°C)	Δ*H* (J/g)	Water %	*T* (°C)	Δ*H* (J/g)	Cryst. %	*T* (°C)	Δ*H* (J/g)
0%	over silica	91	−45.8	2.0	181	−53.7	34.9	220	−9.0	94	−63.5	2.8	178	−46.5	30.2	209	−0.5
44%	2/moist	84	−62.3	2.8	180	−53.8	34.9	222	−9.8	85	−67.2	3.0	179	−33.2	21.6	212	−1.9
	2/dry	88	−34.6	1.5	181	−54.0	35.0	222	−6.6	89	−45.3	2.0	179	−52.0	33.7	206	−0.3
	7/moist	80	−83.0	3.7	181	−44.2	28.7	221	−8.5	87	−82.8	3.7	179	−32.7	21.2	212	−1.5
	7/dry	80	−37.8	1.7	181	−47.7	31.0	219	−8.6	94	−32.8	1.5	179	−36.6	23.8	209	−0.8
65%	2/moist	77	−81.5	3.6	186	−46.2	30.0	222	−10.5	80	−115.6	5.1	179	−35.5	23.0	209	−1.2
	2/dry	83	−35.7	1.6	186	−28.6	18.6	223	−10.3	91	−44.4	2.0	178	−35.5	23.0	212	−1.9
	7/moist	69	−5.2	0.2	185	−77.4	50.3	224	−9.2	79	99.0	4.4	175	−35.2	22.9	209	−0.9
	7/dry	74	−4.7	0.2	185	−80.4	52.2	223	−8.3	92	−34.2	1.5	175	−37.6	24.4	211	−1.7
75%	2/moist	66	−15.3	0.7	189	−95.5	62.0	225	−10.9	91	−165.1	7.3	179	-26.4	17.2	217	−2.1
	2/dry	80	−5.1	0.2	190	−104.6	67.9	227	−10.2	92	−41.9	1.9	178	−51.6	33.5	217	−2.3
	7/moist	68	−14.7	0.7	190	−106.1	68.9	227	−11.0	91	−192.0	8.5	181	−17.0	11.1	221	−1.8
	7/dry	80	−5.0	0.2	190	−106.7	69.3	227	−10.9	103	−18.0	0.8	177	−28.4	18.4	221	−2.6

RH Relative humidity, *T* peak temperature, *ΔH* the enthalpy of endothermic change, *water %* the water content of sample, *cryst. %* the crystallization degree of sample

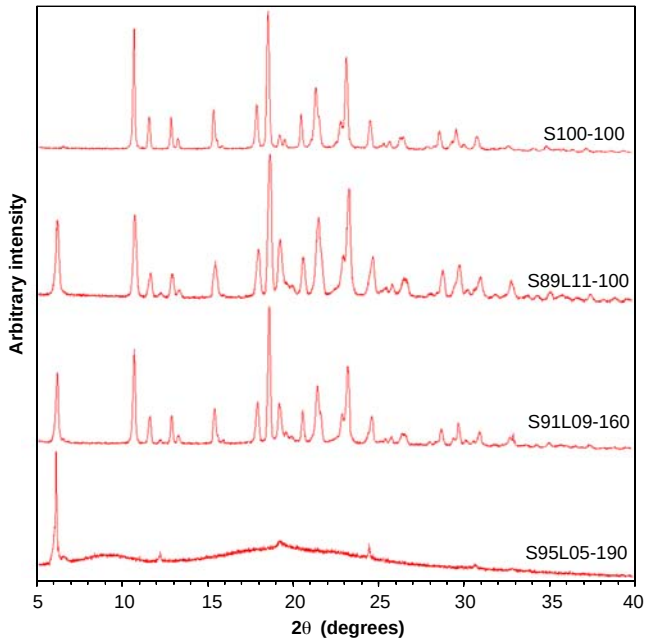

Fig. 7. The XRD spectra of the produced particles S100–100, S89L11–100, S91L09–160, and S95L05–190 after humidification at 65% RH for 7 days and drying over silica for 5 days.

three-fold. A sharp endotherm at the T_{peak} of 202–203°C was indicative of the melting of large-domained crystals that were formed by the fusion of small crystal domains. Two overlapping endotherms in the thermograms (f and j) suggest the coexistence of crystalline domains of different shapes (37). Accordingly, the crystallization process of salbutamol sulphate was assumed to be in an intermediate state where various crystal shapes could coexist. This state was observed particularly with S100–100 where the endotherms fused together indicating a single crystal shape upon the humidity and drying treatment, see Fig. 6. Multiple endotherms in the range 110–190°C has been reported to be due to the degraded products of salbutamol sulphate (41). This could be also related to the crystal melting since the magnitude of the endotherms decreased and shifted to higher temperatures as water was removed by drying. In this case, water acted as a plasticizing agent to decrease the melting temperature. Nevertheless, such multiple endotherms did not appear with the L-leucine-containing particles meaning that L-leucine either prevented this phenomenon to take place or the phenomenon did not existed in these particles. The crystallization of S89L11–100 and S91L09–160 also developed upon conditioning. The extent of the crystallization of S89L11–100 depended only on the relative humidity, whereas in the case of S91L09–160 it depended on both the exposure time and relative humidity, see Table III. The peak temperatures of these samples were lower than 202°C, indicating that the crystals did not form a solid crystalline continuum throughout the particles, but likely still existed as different-sized separated crystalline domains within the amorphous matrix. These domains would be formed by merging of small crystalline domains resulting in crystal size to increase. This was also observed by XRD diffraction where the intensities of diffraction peaks characteristics to crystalline salbutamol increased while narrowed upon humidity treatment, see Fig. 7. The S95L05–190 showed very large water uptake and no crystallization, which agrees well with the DVS results. This outcome was surprising, since regardless of the high water uptake, the salbutamol in S95L05–190 particles did not crystallize. This phenomenon may occur if the molecule has been changed, for instance, upon degradation during the powder preparation. As already discussed, salbutamol sulphate melts with degradation. It was observed in the DSC thermograph of bulky salbutamol sulphate that the onset temperature of the endotherm attributed to melting/degradation was approximately 185°C. Larhrib *et al.* (37) observed that salbutamol sulphate showed no transition from solid to liquid state at 200°C which was understood as molecular degradation without melting. The authors proposed based on the molecular structure that the cleaved group could be *tert*-butylamine. We carried out LC-MS studies with S95L05-190 which evidently showed that salbutamol sulphate had been partially decomposed at 190°C (Supplementary data on LC-MS; further information given by the publisher). The *m*/*z* of 461–463 implicated that *tert*-butyl groups of salbutamol molecules had been cleaved. The structure of the remaining molecule may explain high water uptake upon humidification but no crystallization.

Particles after Thermal Treatment

Figure 8 shows the SEM images of the 0% RH samples after the DSC runs from 25°C to 250°C. One should bear in mind that the decomposition of salbutamol begins above 200°C. After the heat treatment, the S100–100 formed large coagulated structures with no resemblance to the individual particles. Also the appearance of the powder was granulated and the colour was deep red, whereas the powder was pale yellow before the treatment. None of the L-leucine-containing particles agglomerate and they still retained their powdery behaviour. All the

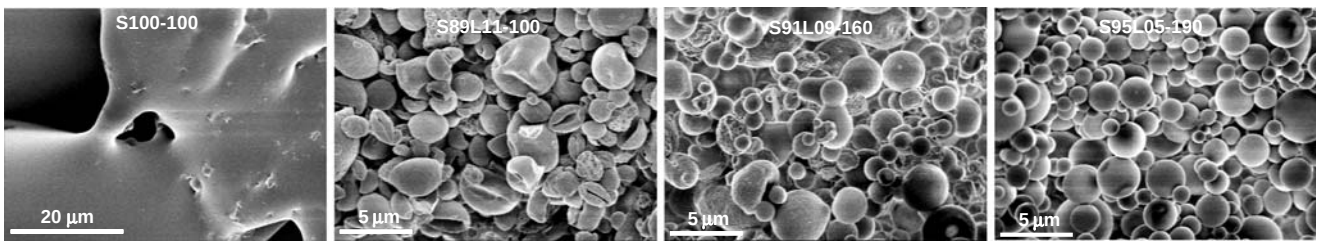

Fig. 8. The SEM images of the samples after the DSC measurements with a heat scan from 25°C to 250°C. The samples are from left to right S100–100, S89L11–100, S91L09–160, and S95L05–190.

samples were yellowish brown, suggesting that salbutamol had decomposed beneath the L-leucine surface layer. Although the crystallization of salbutamol was not initiated and/or boosted by heat in the present case, this particle structure with the L-leucine coating can possibly be applied to molecules that crystallize by thermal means without losing their particle integrity.

Influence of Coating on Particle Stability

Amorphous salbutamol sulphate crystallizes in humid conditions due to the plasticizing effect of water. Once humidified, T_g may be sufficiently lowered for the amorphous material to crystallize. As discussed above, the particle morphology may drastically change during crystallization, leading, for instance, to agglomeration of the particles. In the case of inhalable powders, this agglomeration is a very undesirable phenomenon, since the resulting agglomerate size may not be within the respirable size range. In the present study, pure salbutamol particles without an L-leucine coating crystallized but coagulated heavily in humid conditions. Instead, the L-leucine-coated particles S89L11–100 and S91L09–160 retained their morphology and did not seem to form agglomerates when salbutamol sulphate crystallized. The sample S95L05–190 did not crystallize most probably due to molecular degradation as discussed above but the particles showed strong agglomeration upon humidification. Among the particles, sample S89L11–100, where the coating layer was formed purely by droplet drying (Case 1 in Fig. 1), seemed to give the best protection against particle coagulation, whereas sample S95L05–190, where the coating was formed by vapour deposition (Case 3 in Fig. 1), seemed to be more prone to agglomeration upon exposure to humidity. Water as incorporated in the amorphous region can increase the free volume and the molecular mobility of the solid, which leads to a reduction in the glass-transition temperature. This facilitates the organization of molecules, resulting in 'ordinary' crystals as well as crystalline hydrates if it occurs. In the case of the uncoated salbutamol particles, there was no outer layer to prevent large-scale organization and the particles freely fused together. In contrast, the L-leucine layer prevented (at 65% RH) particle coagulation during the crystallization of salbutamol. It is suggested that water molecules when first absorbed on the particle surface diffused into a less water-containing environment, i.e. through the L-leucine coating into the particle interior via small adducts.

The L-leucine coating also proved to be a very efficient approach to preserving the integrity of the particles even at high temperatures. This is due to the thermal stability of L-leucine in the bulky matrix where heat transfer and related properties differ from those for a single particle. In fact, we have reported that the stability sof L-leucine was not the same when we studied separate, individual particles but that L-leucine could be removed at 200°C in 10 min (32).

CONCLUSIONS

In conclusion, an L-leucine coating on micron-sized salbutamol sulphate particles protects the particle integrity against moisture and high temperatures. At a moisture content of 65% RH, the uncoated salbutamol particles fuse together while the particles with an L-leucine coating preserve their integrity or are slightly sintered. A higher moisture content induces sintering regardless of the type of L-leucine coating. As observed visually, the L-leucine layer formed by diffusion gives better protection than if the L-leucine layer is introduced via vapour deposition. In order to preserve good flowability together with good physical stability, the best coating would contain two L-leucine layers, the inner layer being formed by diffusion (physical stability) and the outer layer by vapour deposition (flowability). Within the particles salbutamol is crystalline to some extent, forming nano-sized crystalline domains beneath the L-leucine layer formed by the diffusion without losing the particle integrity. The structures of the L-leucine-coated particles were also resistant to temperatures up to 250°C, whereas salbutamol particles without a coating strongly fused.

ACKNOWLEDGEMENTS

We thank the Academy of Finland for financial support. Graduate student Raita Heiskanen is thanked for assistance with the experimental work.

REFERENCES

1. G. Buckton, P. Darcy, D. Greenleaf, and P. Holbrook. The use of isothermal microcalorimetry in the study of changes in crystallinity of spray-dried salbutamol sulphate. *Int. J. Pharm.* **116**:113–118 (1995).
2. B. C. Hancock, and G. Zografi. Characteristics and significance of the amorphous state in pharmaceutical systems. *J. Pharm. Sci.* **86**:1–12 (1997)and references therein.
3. R. Surana, A. Pyne, and R. Suryanarayanan. Effect of aging on the physical properties of amorphous trehalose. *Pharm. Res.* **21**:867–874 (2004).
4. N. Rodrigues-Hornedo, D. Lechuga-Ballesteros, and H. J. Wu. Phase transition and heterogeneous/epiaxial nucleation of hydrated and anhydrous theophylline crystals. *Int. J. Pharm.* **85**:149–162 (1992).
5. V. K. Kakumanu, and A. K. Bansal. Enthalpy relaxation studies of Celecoxib amorphous mixtures. *Pharm. Res.* **19**:1873–1878 (2002).
6. M. Yoshioka, B. C. Hancock, and G. Zografi. Inhibition of indomethacin crystallization in poly(vinylpyrrolidone) coprecipitates. *J. Pharm. Sci.* **84**:983–986 (1995).
7. L. Yu, D. S. Mishra, and D. R. Rigsbee. Determination of the glass properties of D-mannitol using sorbitol as an impurity. *J. Pharm. Sci.* **87**:774–777 (1998).
8. N. Y. K. Chew, and H.-K. Chan. Use of solid corrugated particles to enhance powder aerosol performance. *Pharm. Res.* **18**:1570–1577 (2001).
9. N. Y. K Chew, B. Y. Shekunov, H. H. Y. Tong, A. H. L. Chow, C. Savage, J. Wu, and H.-K. Chan. Effect of amino acids on the dispersion of disodium cromoglycate powders. *J. Pharm. Sci.* **94**:2289–2300 (2005).
10. A. M. Abdul-Fattah, V. Truong-Le, L. Yee, E. Pan, Y. Ao, D. S. Kalonia, and M. J. Pikal. Drying-induced variations in physico-chemical properties of amorphous pharmaceuticals and their impact on stability II: Stability of a vaccine. *Pharm. Res.* **24**:715–727 (2007).
11. J. Calderon De Anda, X. Z. Wang, X. Lai, and K. J. Roberts. Classifying organic crystals via in-process image analysis and the use of monitoring charts to follow polymorphic and morphological changes. *J. Process Control.* **15**:785–797 (2005).
12. J.-F. Willart, J. Lefebvre, F. DanèIde, S. Comini, P. Looten, and M. Descamps. Polymorphic transformation of the G-form of d-sorbitol upon milling: structural and nanostructural analyses. *Solid State Commun.* **135**:519–524 (2005).

13. D. Begon, P. Guillaume, and M. Kohl. Process for producing fine medicinal substances. *WO World IPO 0114036* (2001).
14. R. W. Lancaster, H. Sigh, and A. L. Theophilus. Apparatus and process for preparing crystalline particles. *WO World IPO 0038811* (2000).
15. B. Y. Shekunov, S. Bristow, A. H. L. Chow, L. Cranswick, D. J. W. Grant, and P. York. Formation of composite crystals by precipitation in supercritical CO_2. *Cryst. Growth Des*. **3**:603–610 (2003).
16. L.-E. Briggner, K. Bystrom, E. Jakupovic, E. Trofast, and J. Trofast. Pharmaceutical formulation. *US Patent 5,874,063* (2002).
17. B. Hancock, and G. Zografi. The relationship between the glass transition temperature and the water content of amorphous pharmaceutical solids. *Pharm. Res*. **11**:471–477 (1994).
18. K. D. Kussendrager, and M. J. H. Ellison. Carrier material for dry powder inhalation. *WO 02/07705* (2002).
19. G. H. Ward, and R. K. Schultz. Process-induced crystallinity changes in albuterol sulfate and its effect on powder physical stability. *Pharm. Res*. **12**:773–779 (1995).
20. K. Dick, T. Dhanasekaran, Z. Zhang, and D. Meisel. Size-dependent melting of silica-encapsulated gold nanoparticles. *J. Am. Chem. Soc*. **124**:2312–2317 (2002).
21. J. Raula, A. Kuivanen, A. Lähde, and E. I. Kauppinen. Gas-phase synthesis of L-leucine-coated micrometer-sized salbutamol sulphate sodium chloride particles. *Powder Technol.*, DOI 10.1016/j.powtec.2008.03.006 (2008).
22. J. Glinski, G. Chavepeyer, and J.-K. Platten. Surface properties of aqueous solutionss of L-leucine. *Biophys. Chem*. **84**:99–103 (2000).
23. N. Matubayasi, H. Miyamoto, J. Namihira, K. Yano, and T. Tanaka. Thermodynamic quantities of surface formation of aqueous electrolyte solutions V. Aqueous solutions of aliphatic amino acids. *J. Colloid Interface Sci*. **250**:431–437 (2002).
24. J. Raula, A. Lähde, and E. I. Kauppinen. A novel gas phase method for the combined synthesis and coating of pharmaceutical particles. *Pharm. Res.* **25**:242–245 (2008).
25. H. Eerikäinen, W. Watanabe, E. I. Kauppinen, and P. P. Ahonen. Aerosol flow reactor method for synthesis of drug nanoparticles. *Eur. J. Pharm. Biopharm*. **55**:357–360 (2003).
26. J. Raula, H. Eerikäinen, and E. I. Kauppinen. Influence of the solvent composition on the morphology of polymer drug composite nanoparticles. *Int. J. Pharm*. **284**:13–21 (2004).
27. Y. Zhu, and K. W. Lee. Experimental study on small cyclones operating at high flow rates. *J. Aerosol Sci*. **30**:1303–1315 (1999).
28. H. J. Svec, and D. D. Clyde. Vapour pressures of some alpha-amino acids. *J. Chem. Eng. Data*. **10**:151–152 (1965).
29. F. P. Incropera, and D. P. DeWitt. *Fundamentals of Heat and Mass Transfer. 5*Wiley, New York, 2002, pp. 846–847.
30. R. J. Lang. Ultrasonic atomization of liquids. *J. Acoust. Soc. Am*. **1**:6 (1962).
31. R. C. Flagan, and J. H. Seinfeld. *Fundamentals of Air Pollution Engineering*. Prentice Hall, Englewood Cliffs, 1988, p. 542.
32. J. Raula, J. A. Kurkela, D. P. Brown, and E. I. Kauppinen. Study of the dispersion behaviour of L-leucine containing microparticles synthesized with an aerosol flow reactor method. *Powder Technol*. **177**:125–132 (2007).
33. J. Raula, A. Kuivanen, A. Lähde, and E. I. Kauppinen. Synthesis of L-leucine nanoparticles via physical vapor deposition under various saturation conditions. *J. Aerosol Sci.* **38**:1172–1184 (2007).
34. A. Columbano, G. Buckton, and P. Wikeley. A study of the crystallisation of amorphous salbutamol sulphate using water vapour sorption and near infrared spectroscopy. *Int. J. Pharm*. **237**:171–178 (2002).
35. D. J. Burnett, F. Thielmann, and J. Booth. Determining the critical relative humidity for moisture-induced phase transitions. *Int. J. Pharm*. **287**:123–133 (2004).
36. G. Buckton, and P. Darcy. The use of gravimetric studies to assess the degree of crystallinity of predominantly crystalline powders. *Int. J. Pharm*. **123**:265–271 (1995).
37. H. Larhrib, G. P. Martin, C. Marriott, and D. Prime. The influence of carrier and drug morphology on drug delivery from dry powder formulations. *Int. J. Pharm*. **257**:283–296 (2003).
38. T. S. Martins, J. R. Matos, G. Vicentini, and P. C. Isolani. Synthesis, characterization, spectroscopy and thermal analysis of rare earth picrate complexes with L-leucine. *J. Therm. Anal. Calorim*. **86**:351–357 (2006).
39. J. Li, Z. Wang, X. Yanga, L. Hua, Y. Liu, and C. Wang. Decomposing or subliming? An investigation of thermal behavior of L-leucine. *Thermochim. Acta*. **447**:147–153 (2006).
40. S. Budavari, M. J. O'Neil, A. Smith, and P. E. Heckelman (Eds.). *The Merck Index, 11th edn.*, Rahway, USA, 1989, p. 857.
41. D. O. Corrigan, O. I. Corrigan, and A. M. Healy. Predicting the physical state of spray dried composites: salbutamol sulphate/lactose and salbutamol sulphate/polyethylene glycol co-spray dried systems. *Int. J. Pharm*. **273**:171–182 (2004).
42. H. Eerikäinen, L. Peltonen, J. Raula, E. I. Kauppinen, and J. Hirvonen. Nanoparticles containing ketoprofen and acrylic polymers prepared by an aerosol flow reactor method. *AAPS Pharm. Sci. Tech*. **5**:68 (2004).
43. Q. Jiang, H. X. Shi, and M. Zhao. Melting thermodynamics of organic nanocrystals. *J. Chem. Phys*. **111**:2176–2180 (1999).
44. Q. Jiang, Z. Zhang, and J. C. Li. Melting thermodynamics of nanocrystals embedded in a matrix. *Acta Mater.* **48**:4791–4795 (2000).
45. S. L. Lai, J. Y. Guo, V. Petrova, G. Ramanath, and L. H. Allen. Size-dependent melting properties of small tin particles: nanocalorimetric measurements. *Phys. Rev. Lett*. **77**:99–102 (1996).
46. M. Zhao, and Q. Jiang. Melting and surface melting of low-dimensional In crystals. *Solid State Commun*. **130**:37–39 (2004).
47. D. V. Talapin, A. L. Rogach, A. Kornowski, M. Haase, and H. Weller. Highly luminescent monodisperse CdSe and CdSe/ZnS nanocrystals synthesized in a hexadecylamine–trioctylphosphine oxide–trioctylphospine mixture. *Nanoletters*. **1**:207–211 (2001).
48. A. M. Abdul-Fattah, K. M. Dellerman, R. H. Bogner, and M. J. Pikal. The effect of annealing on the stability of amorphous solids: chemical stability of freeze-dried moxalactam. *J. Pharm. Sci*. **96**:1237–1250 (2007).
49. J. Liu, D. R. Rigsbee, C. Stotz, and M. J. Pikal. Dynamics of pharmaceutical amorphous solids: the study of enthalpy relaxation by isothermal microcalorimetry. *J. Pharm. Sci*. **91**:1853–1862 (2002).
50. V. B. Pokharkar, L. P. Mandpe, M. N. Padamwar, A. A. Ambike, K. R. Mahadik, and A. Paradkar. Development, characterization and stabilization of amorphous form of a low T_g drug. *Powder Technol*. **167**:20–25 (2006).